ORIGINAL PAPER

Characterization of changes in structural, physicochemical and mechanical properties of rigid polyurethane building insulation after thermal aging in air and seawater

Izabela Barszczewska-Rybarek[1] · Katarzyna Jaszcz[1] · Grzegorz Chladek[2] ·
Paulina Grabowska[1] · Agnieszka Okseniuk[1] · Michalina Szpot[1] ·
Magdalena Zawadzka[1] · Aleksandra Sokołowska[2] · Aleksandra Tarkiewicz[2]

Abstract

The purpose of this study was the identification of qualitative and quantitative changes in the visual appearance, chemical structure, morphology and selected physicochemical and mechanical properties of the closed cell rigid PU foam while heated in air and seawater for predicting its performance and durability. Specimens were aged at constant temperatures of 40 and 80 °C for a period of 10 weeks. Aging caused a yellowing of the samples. Scanning electron microscopy (SEM) revealed that foam pores lost their regularity. Differential scanning calorimetry (DSC) showed that the glass transition temperature (T_g) increased on average by 15 and 80%, respectively for samples heated at 40 and 80 °C. Water absorption (WS) also increased over time, respectively, by a maximum of 15 and 25%. The flexural strength (σ_{flex}) and compressive (σ_{comp}) strength showed a decreasing tendency, whereas for tensile strength (σ_{tens}), an increase was observed. The starting material was characterized by the σ_{flex}, σ_{tens} and σ_{comp} of: 436, 413 and 284 kPa, respectively. The lowest determined σ_{flex} value was of 345 kPa, and σ_{comp} value was of 158 kPa. The highest determined σ_{tens} equaled to 608 kPa, respectively. The changes in flexural modulus were statistically insignificant and its average value was of 4.0 MPa.

✉ Izabela Barszczewska-Rybarek
Izabela.Barszczewska-Rybarek@polsl.pl

[1] Department of Physical Chemistry and Technology of Polymers, Silesian University of Technology, M. Strzody 9, 44-100 Gliwice, Poland

[2] Institute of Engineering Materials and Biomaterials, Silesian University of Technology, Gliwice, Poland

Introduction

In recent years, the discussion on problems of modern building construction is dominated by issues related to the maximization of energy efficiency and minimalization of the negative impact on the environment. The rigid polyurethane (PU) foams offer the best solution for these problems [1, 2]. PU insulations are commonly used in many building applications, such as insulation panels, roofing sandwich panels, spray and injection insulation, pre-insulated pipes [3]. When compared to other popular thermal insulating materials, such as expanded polystyrene and mineral wool, they provide a splendid thermal insulation performance. They have the lowest thermal conductivity. Thus, a significant reduction in the insulation thickness and weight can be achieved. It is reflected in the lower costs of insulating material used, the space saved inside the building as well as lower amounts of post-consumer waste, which require utilization. The rigid PU foam is very durable, difficult to deform, has low water absorption and is resistant to a wide spectrum of chemicals. Additionally, the spray PU foam application process reduces the formation of thermal bridges to a minimum, it is easy, quick, free from harmful dusts and fibers [3–6].

The industry is interested in the high quality of the PU insulations offered, which must meet a number of physicochemical and mechanical requirements. In particular, the stability of those properties throughout the service life is crucial. Comprehensive studies can enable a thorough explanation and understanding of these properties and their changes as a result of environmental factors, such as elevated temperature, seawater, UV irradiation. The knowledge gained can be used in the identification and prediction of the causes of polyurethane insulation failure during its handling.

The influence of environmental factors on the stability of physicochemical and mechanical properties of commercial PU foams is rarely the subject of research. Marrucho et al. [7] tested thermal conductivity of closed cell polyurethane foams, formed with the use of three nitrogen/cyclopentane mixtures, at temperatures between 315 and 396 K and pressures up to 0.53 MPa. The experimental thermal conductivity data were correlated with the Wassiljewa mixing rules and predicted using extended corresponding states theory (ECST). They found that the increase in the nitrogen fraction in the cyclopentane–nitrogen mixture leads to higher thermal conductivity values than those predicted by ECST. Davies et al. [8] examined commercial polyether-based polyurethanes for use in underwater applications. Two PU samples, characterized by 40 and 90 Shore A hardness, have been subjected to immersion in artificial seawater for periods up to 2 years at temperatures from 50 to 100 °C. The results showed that tested materials retain 100% of their initial tensile properties after 5 years of immersion. However, the FTIR analysis indicated that hydrolysis can occur. Liszkowska et al. [9] tested two series of rigid polyurethane-polyisocyanurate foams (with and without flame retardant) obtained from commercial components and modified with cinnamon extract. They were subjected to degradation, acting on samples a defined temperature, humidity and UV radiation (respectively, 50 °C, 70%, 320.86 W/m^2) for 7 days. Conditioning

resulted in an increase in the red color of foams, decrease in compressive strength from 15 to 42% (in the series with flame retardant) and from 66 to 75% (in the series without flame retardant), decrease in brittleness from 13 to 11% (in the series with flame retardant) and an increase from 16 to 45% (in the series without flame retardant). Changes in the chemical structure and morphology were found too. The urethane bond destruction was detected utilizing infrared spectroscopy (FTIR), whereas the partial cell opening was observed in SEM images. In another study, Liszkowska et al. [10] tested photodegradation and biodegradation of polyurethane-polyisocyanurate foams modified with cinnamon extract, green coffee extract and cocoa extract in an amount of 10 wt.%. Photodegradation was performed at 50 °C, 70% relative humidity and UV irradiance of 320.86 W/m^2 for 7, 14, and 21 days, whereas biodegradation was performed in a soil environment for 28 days. The results showed that the addition of coffee and cocoa extract increased the aging resistance of foams in comparison to unfilled foam and foam with cinnamon extract. The decreases in compressive strength were similar for each type of degraded foam and, on average, they corresponded to 49%. Biodegradation tests showed that foams modified with plant-based fillers were more susceptible to biodegradation than the unfilled foam.

In this study, the identification of qualitative and quantitative changes in the visual appearance, chemical structure, morphology, selected physicochemical and mechanical properties of commercial PU rigid foam while heated in the air and seawater was performed for predicting its performance and durability. Specimens of the closed cell rigid PU foam were aged at constant temperatures of 40 and 80 °C for a period of 10 weeks. The chemical structure was analyzed utilizing attenuated total reflectance-Fourier transform infrared spectroscopy (ATR-FTIR). Changes in morphology were observed with the use of SEM, whereas changes in thermal properties were analyzed by DSC. Dimensional changes, water absorption and selected mechanical properties, such as tensile strength, compressive strength, flexural strength and flexural modulus were also analyzed.

Experimental

Material

The samples were prepared at a construction site while spraying polyurethane insulation on the building roof. The commercial closed cell rigid polyurethane system Synthesia Internacional (Barcelona, Spain) was applied. For the purpose of this work, the foam was sprayed on a board substrate in the layer thickness of 6 cm. Testing specimens were cut from that material with the use of two saw blades that differed in blade diameter (25 and 12 cm) and cutters (used for the preparation of disc-like and dumbbell-shaped samples). Before testing, they were sanded clean with fine sanding paper until smooth, level surfaces were obtained. Then, specimens were blown-off with the compressed air to remove all the loose particles from their surfaces. The rectangular specimens of 130 mm×40 mm×20 mm (length×width×thickness) were prepared for testing flexural properties, cubes of

40 mm×40 mm×40 mm were prepared for testing compressive strength, dumbbell-shaped samples of 75 mm×4 mm×2 mm (length×parallel section width×thickness) were prepared for testing tensile strength and discs of 20 mm×3 mm (diameter×thickness) were prepared for testing dimensional changes, mass changes and water absorption. The latter specimens were also used for ATR-FTIR, DSC and SEM analyses.

Density measurement

The foam density was measured utilizing an analytical balance with a 0.01 mg accuracy (XP Balance, Mettler Toledo, Greifensee, Switzerland) equipped with a density determination kit. Water was used as an immersion liquid.

Aging

Aging of PU foams was performed in air circulated laboratory ovens at 40 and 80 °C for a maximum duration of 10 weeks. Samples were tested in two environments: air and seawater at both temperatures. Therefore, four sample series were analyzed: aged at 40 °C in the air, aged at 80 °C in the air, aged at 40 °C in the seawater and aged at 80 °C in the seawater. Samples aged in air were placed on Petri dishes on supports allowing air circulation around the sample. Samples aged in seawater were placed in sealed vessels containing artificial seawater prepared according to ASTM D1141 [11]. Since PU foam is lighter than water and floats onto its surface, a sinker was used to ensure full sample immersion. For this purpose, pouches were sewn from medical gauze, in which samples and glass weights were placed. Samples were taken out every 2 weeks and tested. Air-aged samples were tested immediately after stabilizing at room temperature. The seawater-aged samples were washed with distilled water and dried in a vacuum oven at 40 °C until constant weight was achieved. The testing of water absorption was performed without vacuum drying, as an exception. Instead, samples were paper towel-dried before testing.

Dimensional changes

The dimensional changes were determined according to the ISO 1923:1981 standard [12]. Disc-like specimens, aged in the air environment were used in these tests. The 0–150 mm caliper, with a 0.01 mm accuracy, was used in this measurement. Before aging, each sample was measured for diameter and length. The initial diameter was designated as (D_0), whereas the initial thickness was designated as (d_0). Then, the samples were placed in the ovens for 2, 4, 6, 8 and 10 weeks at 40 and 80 °C. After these time intervals, the three samples were removed from the ovens, stabilized at room temperature and tested for dimensions, respectively, diameter (D) and thickness (d). The percentage changes in diameter (ΔD) and thickness (Δd) were calculated using the following equations:

$$\Delta D \,(\%) = 100 \times \frac{D_0 - D}{D} \tag{1}$$

$$\Delta d \,(\%) = 100 \times \frac{d_0 - d}{d} \tag{2}$$

where D_0 is the initial sample diameter, D—the sample diameter after removal from the oven, d_0—the initial sample thickness, d—the sample thickness after removal from the oven.

Mass changes and water absorption

The mass loss (Δm) and water absorption (WS) were determined according to the ISO 2896:2001 standard [13]. Disc-like specimens were used in these measurements utilizing analytical balance, with a 0.01 mg accuracy (XP Balance, Mettler Toledo, Greifensee, Switzerland).

The mass loss was determined for samples aged in the air environment. Before aging each sample was weighed (m_0). Then, the samples were placed in the ovens for 2, 4, 6, 8 and 10 weeks at 40 and 80 °C. After these time intervals, the three samples of each series were removed from the ovens, stabilized at room temperature and weighed (m). The percentage change in sample mass (Δm) was calculated using the following equation:

$$\Delta m \,(\%) = 100 \times \frac{m_0 - m}{m} \tag{3}$$

where m_0 is the initial sample mass, m—the sample mass after removal from the oven.

The water absorption was determined for samples aged in the seawater environment. Before immersing in seawater each sample was dried at 100 °C in a conditioning oven until a constant weight was achieved and weighed (m_0). Then, the samples were immersed in seawater and placed in the ovens for 2, 4, 6, 8 and 10 weeks at 40 and 80 °C. After these time intervals, the three samples were removed from the ovens, washed with distilled water, blotted dry and weighed (m). The water absorption (WS) was calculated using the following equation:

$$WS \,(\%) = 100 \times \frac{m - m_0}{m_0} \tag{4}$$

where m_0 is the dried sample mass, m—the swollen sample mass.

Proton nuclear magnetic resonance spectroscopy (1H NMR)

1H NMR spectra of the polyol and diisocyanate were recorded in the deuterated chloroform solution, using tetramethylsilane (TMS) as an internal standard. A 300 MHz NMR spectrometer (UNITY/INOVA, Varian, Palo Alto, CA, USA) was employed for these experiments.

The glycol molar ratio in the polyol was determined by the relative area of the 1H NMR signals.

The ethylene glycol mole fraction was calculated according to the following equation:

$$\text{EG mole\%} = \frac{\text{EG relative moles} \times 100\%}{\text{EG relative moles} + \text{PG relative moles}} \qquad (5)$$

where EG is ethylene glycol, PG—propylene glycol. The PG and EG relative moles were calculated according to the following equations:

$$\text{PG relative moles} = \frac{\text{integral for CH}_3 \text{ protons}}{3} \qquad (6)$$

where 3 corresponds to the number of protons in the methyl group ($-CH_3$).

$$\text{EG relative moles} = \frac{\text{integral for CH}_2 \text{ and CH protons - integral for CH}_3 \text{ protons}}{4} \qquad (7)$$

where 4 corresponds to the number of protons in the methylene groups ($-CH_2-$) in EG.

Attenuated total reflectance-Fourier transform infrared spectroscopy (ATR-FTIR)

ATR-FTIR spectra were recorded at room temperature in the range between 400–3600 cm^{-1} utilizing a Spectrum Two (PerkinElmer, Waltham, MA, USA) spectrometer. The spectra were recorded with 32 scans at a resolution of 4 cm^{-1}.

Differential scanning calorimetry (DSC)

The calorimetric measurements were carried out on a differential scanning calorimeter DSC 822^e (Mettler Toledo, Greifensee, Switzerland). Samples of 2.08 ± 0.03 mg were heated from 0 to 350 °C with a heating rate 10 K/min in the air. The glass transition temperature (T_g) was taken as the midpoint on the slope of the baseline shifting resulted from the glass transition, according to ISO 11357–2:2020 [14].

Scanning electron microscopy (SEM)

Morphology investigations were performed with the Phenom Pro Desktop SEM (Thermo Scientific, Waltham, MA, USA). The sample surfaces, before the observations, were sputter coated with gold layer 10 nm thick. Images were recorded at 250, 500 and 1500 times magnification.

Mechanical testing

The tests of mechanical properties were carried out on a universal testing machine Z050 (Zwick, Ulm, Germany). The measurement was repeated three times for

each measured property: flexural strength and modulus, tensile strength and compressive strength. For comparison purposes, the original sample was also tested. Flexural strength (σ_{flex}) and modulus (E) were measured on the rectangular samples 130 mm×40 mm×20 mm (length×width×thickness), according to PN-EN 12,089:2013 [15]. Tensile strength (σ_{tens}) was measured on the dumbbell-shaped samples of 75 mm×4 mm×2 mm (length×parallel section width×thickness), according to PN-EN 1608 (2013) [16]. Compressive strength (σ_c) was measured on the cubic samples of 40 mm×40 mm×40 mm (length×width×thickness), according to PN-EN 826:2013 [17].

Results

The studied PU foam was formed by reacting a diisocyanate with a polyol during the spray process. Before spraying, the monomer samples were taken in order to identify their chemical composition. 1H NMR spectroscopy was utilized for this purpose. As shown in Fig. 1, the diisocyanate component was 4,4′-diphenylmethane diisocyanate (MDI), which gives a singlet of methylene group at 3.88 ppm (2 protons) and two doublets of two phenylene rings (4 protons each doublet) at 6.97 and 7.07.

As shown in Fig. 2, the polyol component was a copolymer of ethylene and propylene glycols (respectively, EG and PG). It gives a multiplet of the PG methyl group at around 1.14 ppm (3 protons) and a series of multiplets of methylene and methine groups coming from EG and PG in the range from 3.65 to 3.43 ppm.

The EG and PG mole fractions were calculated using integral values, according to the equations from 5 to 7. The EG/PP mole ratio was found of 23.45:76.55.

Based on the above, the reaction leading to the formation of the studied polyurethane is shown in Scheme 1.

The studied polyurethane foam was also tested for density and morphology. It was characterized by an average density of 0.047 ± 0.001 g/cm^3. SEM analysis revealed that the foam had a closed cell morphology (Fig. 3).
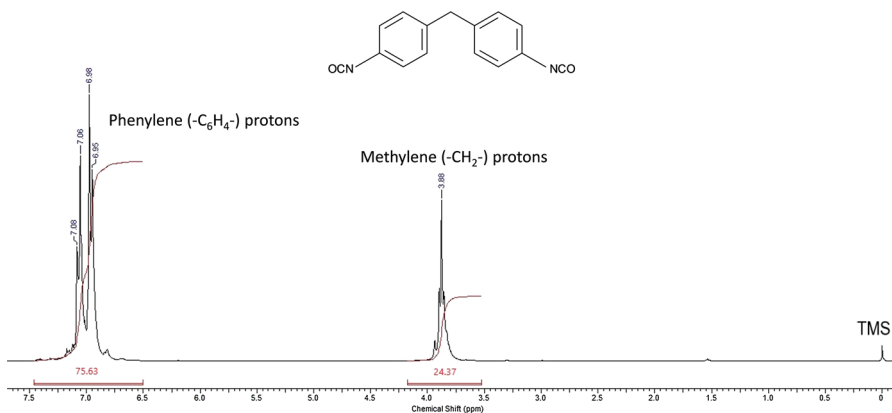

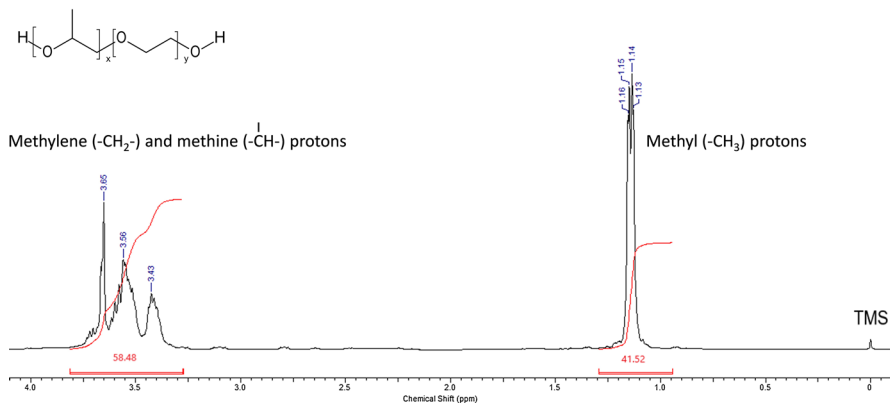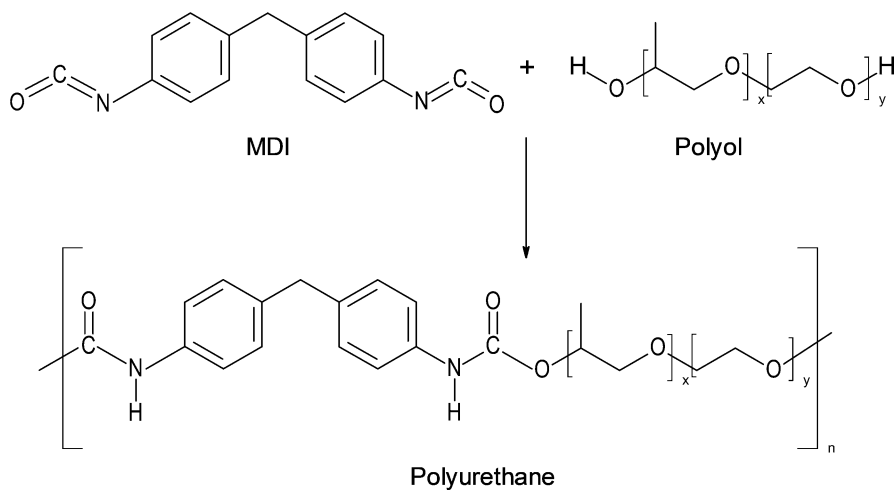**Fig. 1** 1H NMR spectrum of the diisocyanate component

Fig. 2 1H NMR spectrum of the polyol component

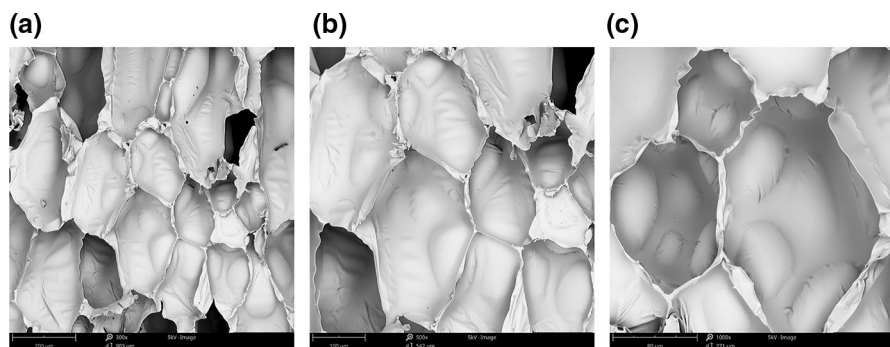Scheme 1 Chemical structure of studied polyurethane

Fig. 3 SEM images of the original PU foam at magnifications: **a** 300x, **b** 500x, **c** 1000x

The PU foam was subjected to aging for a maximum time of 10 weeks at 40 and 80 °C in air and seawater to investigate changes in selected physicochemical and mechanical properties.

The changes in color and surface roughness were observed in aged samples compared to the non-aged one. In Fig. 4, the results of this analysis are shown for samples aged for 2 and 10 weeks.

The original PU foam sample was light straw-colored. It can be seen that the temperature of 40 °C did not significantly affect the sample appearance. Until the end of the experiment duration, i.e., 10 weeks, the samples, heated at 40 °C did not change their color and roughness. Aging at 80 °C caused a slight yellowing of foams after only 2 weeks. By 10 weeks the yellowing had significantly increased and turned to a yellowish-brown. The surface roughness also increased after that time. Seawater caused more intense yellowing.

The PU foam was tested for the stability of linear dimensions. The results showed that its aging caused a reduction in sample linear dimensions. The character and scale of changes depended on the measured dimension, aging temperature and environment. Greater decreases were found for sample diameter than thickness, temperature of 80 °C than 40 °C and seawater environment than the air. The results for samples aged in the air did not show any correlation with time, whereas those for samples aged in seawater showed an exponential correlation with time. The longer the heating time, the greater the reduction in diameter as well as in thickness (Fig. 5). The average decrease in thickness for samples aged in the air at 40 and 80 °C corresponded to $0.47 \pm 0.19\%$, whereas the average decrease in diameter was of $0.05 \pm 0.03\%$. In the case of the seawater-aging, the reduction in thickness ranged from 1.21 to 4.58% for samples aged at 40 °C and
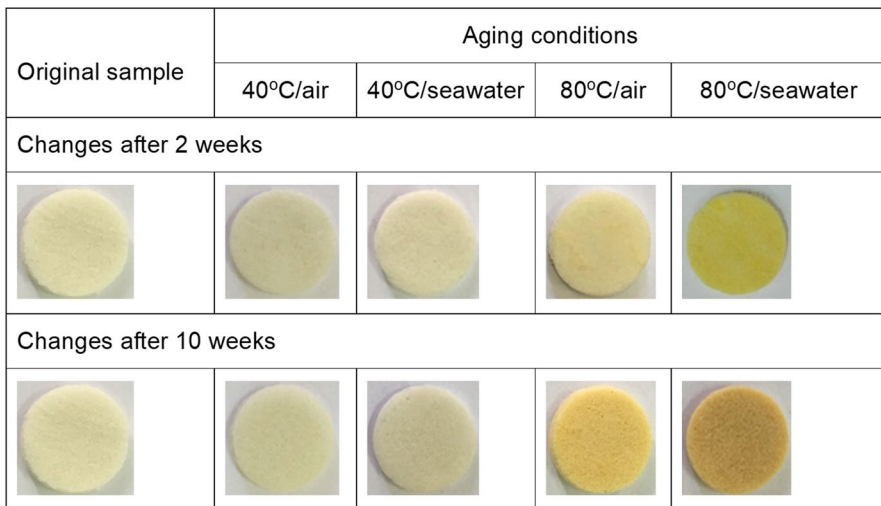

Original sample	Aging conditions			
	40°C/air	40°C/seawater	80°C/air	80°C/seawater
Changes after 2 weeks				
Changes after 10 weeks				

Fig. 4 Visual changes in the PU foam caused by aging at 40 and 80 °C in the air and seawater for 2 and 10 weeks
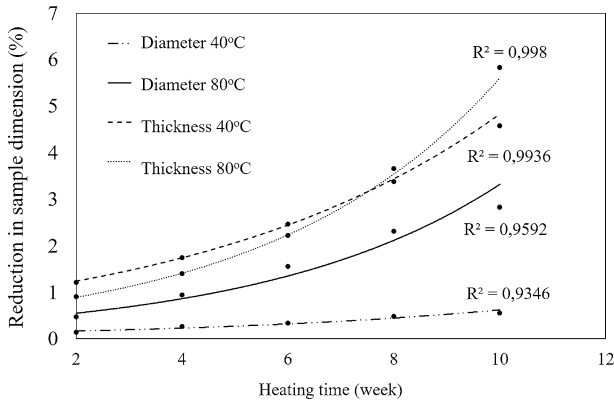
Fig. 5 Relationships between the reduction in sample linear dimensions and the aging time for samples aged in seawater

from 0.91 to 5.83% for samples aged at 80 °C. The reductions in diameter ranged, respectively from 0.14 to 0.55% and from 0.47 to 2.83%.

Samples aged in the air were tested for mass stability. Heating of PU foam in the air resulted in a reduction in sample mass. The decrease scale depended on the heating temperature and was significantly greater for aging at 80 °C (Fig. 6). Heating at 40 °C resulted in a gradual increase in the mass reduction from 1.66% (for samples heated for 2 weeks) to 2.08% (for samples heated for 10 weeks). Heating at 80 °C resulted in a radical mass reduction after 2 weeks of heating, which remained constant during further heating until the end of the experiment duration. The average mass loss observed for those samples corresponded to $5.36 \pm 0.21\%$.

Samples heated in seawater were tested for water absorption. For comparison purposes, the WS of the starting foam was tested too. The results of these measurements are shown in Fig. 7. As can be seen, the foam before aging was characterized
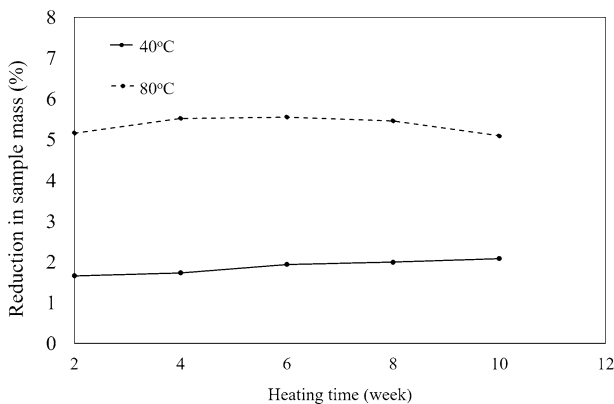

Fig. 6 Relationships between the reduction in sample mass and the aging time for samples aged in the air
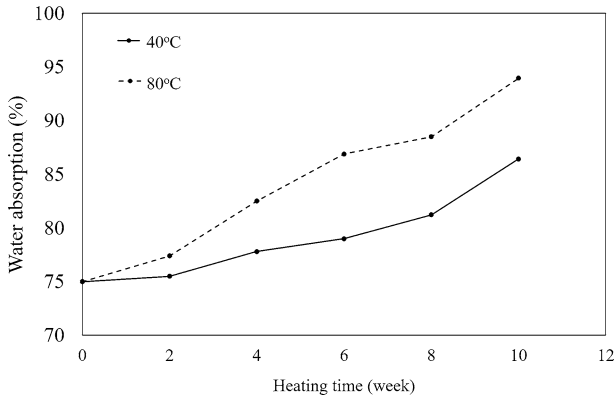
Fig. 7 Relationships between the water absorption and the aging time

by the WS of 75.0%. The aging resulted in the gradual increases in the WS values. Heating at 40 °C resulted in the WS value from 75.5% (for samples aged for 2 weeks) to 86.4% (for samples aged for 10 weeks). Heating at 80 °C resulted in the greater increases in the WS values, which ranged, respectively from 77.4 to 93.9%.

The original sample of the PU foam was subjected to DSC testing. As shown in Fig. 8, heating the starting foam to the temperature of 350 °C revealed the occurrence of the following processes: the glass transition ($T_g = 59.50$ °C), exothermic
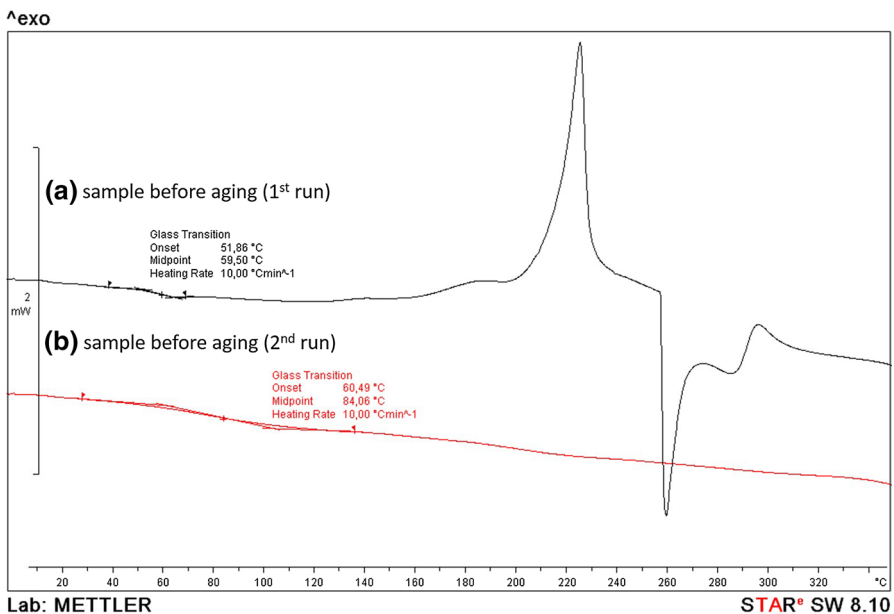

Fig. 8 Comparison of the DSC thermograms, representing the first and second heating runs of an original PU foam
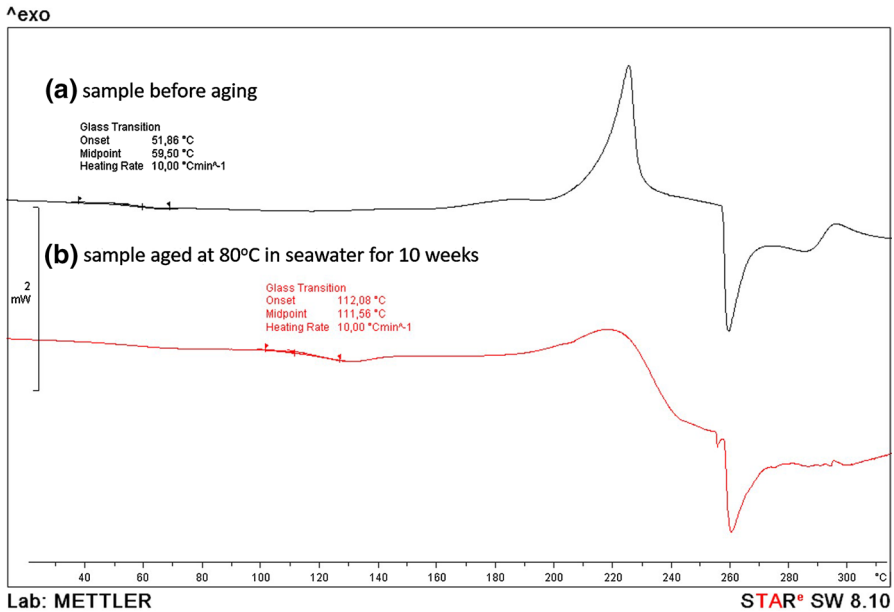
^exo

Fig. 9 Comparison of the DSC thermograms of an original PU foam and the foam aged in seawater at 80 °C for 10 weeks
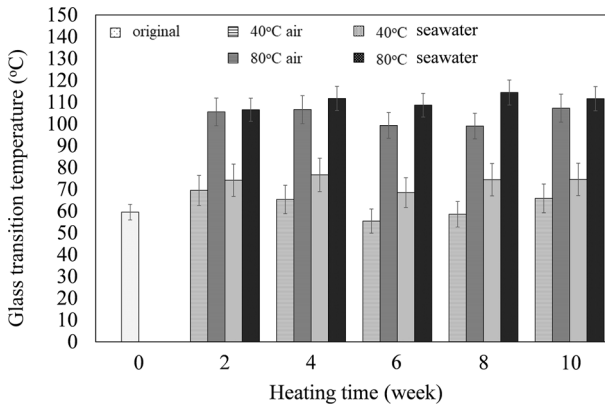

Fig. 10 Glass transition temperature of tested samples

process ($T_{max} = 225$ °C), endothermic process ($T_{min} = 259$ °C) and less pronounced endo- and exothermic processes above 270 °C. The thermogram of the second heating run showed a shift of T_g to a higher value ($T_g = 84.06$ °C) and the disappearance of peaks corresponding to exo- and endothermic processes.

Figures 9 and 10 show the results of DSC tests on the aged PU foams. Figure 9 shows an exemplary change in the T_g value that occurred after 10 weeks of aging of the PU foam at 80 °C in seawater. Figure 10 summarizes the set of results for T_g.

As shown in Figs. 9 and 10, aging caused the T_g increase. Figure 10 shows that the temperature had a much stronger effect on T_g than the environment and time. Just after two weeks of aging, the T_g values increased and achieved a certain level, specific for the particular aging conditions: temperature and environment. Further heating did not cause significant changes in the T_g value. The average T_g value that was observed for the samples aged at 40 °C in the air was the lowest and was of 62.9 ± 5.7 °C, which compared to the T_g of the original sample corresponded to a 6% increase. The average T_g value of the samples aged at 40 °C in seawater was higher and was of 73.6 ± 3.0 °C, which compared to the T_g of the original sample corresponded to a 24% increase. Heating the samples at 80 °C (regardless the environment) resulted in an almost twofold increase in T_g in the relation to the T_g of original sample. The average T_g value of the air-aged samples was of 103.5 ± 4.0 °C, whereas that of the seawater-aged samples was of 110.5 ± 3.1 °C. These average values of T_g corresponded to the increases in, respectively, 74 and 86% when compared to the starting material.

Figure 9 also shows that heating did not cause significant changes in the position and intensity of the remaining peaks present in the DSC thermograms—resulting from the exo- and endothermic processes above the glass transition.

The chemical structure of tested PU foam was investigated utilizing ATR-FTIR. In Fig. 11, the spectra of the starting PU foam and sample aged at 80 °C in the air for 10 weeks are presented. The stretching and bending vibrations of the N–H bonds appeared, respectively, as a broadened band at 3313 cm^{-1} and a strong band at 1512 cm^{-1}. The stretching vibrations of the C=O carbonyl group of the urethane linkage revealed as a strong band at 1712 cm^{-1}. The intense band at 1597 cm^{-1} results from the presence of stretching skeletal vibrations of C=C bonds in the aromatic rings, resulting from the presence of MDI in the structure of the tested PU. The presence of relatively weak bands at 2929 and 2856 cm^{-1} are due to the symmetric and asymmetric stretching vibrations of –CH$_2$– aliphatic groups, resulting
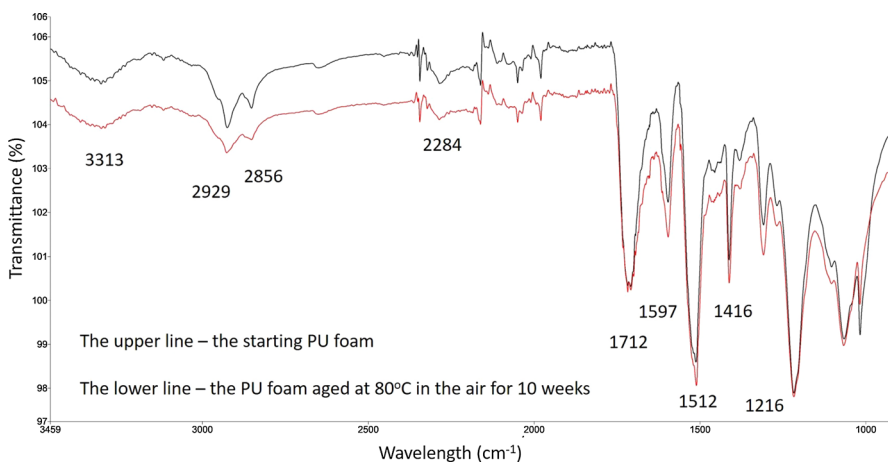

Fig. 11 Comparison of the ATR-FTIR spectra of an original PU foam sample and the foam aged in the air at 80 °C for 10 weeks

from the polyol segment present in the structure of tested PU. The deformation vibrations of the C–H are observed at 1416 cm^{-1}. The band at 1216 cm^{-1} corresponds to the stretching vibration of C(O)O–C groups. The absorption band at 2284 cm^{-1} corresponds to the residual isocyanate groups (N=C=O), which indicates incomplete conversion of the diisocyanate. The insignificant differences were not observed between the non-aged and aged samples.

The morphology of tested PU foam was monitored with the use of SEM. Figure 12 shows a series of SEM images of the starting PU foam and the samples subjected to aging at 40 and 80 °C in the air and seawater for 2 and 10 weeks. The original sample morphology can be recognized as homogeneous, with flat and smooth pore walls. However, bulges can be noticed in the cell walls. The time had a decisive effect on the destruction process of the studied PU foam morphology. The aging at the temperature of 40 °C as well as 80 °C led to similar damages: the cracking of cell edges, which generated crumbs, collection of crumbs at the cell bottoms, cracking of the ribs. This process continued with time, but it was slower at 40 °C. A certain amount of bulges, observed in the starting foam, were still visible in the aged samples, but they radically increased in size and became more pronounced.
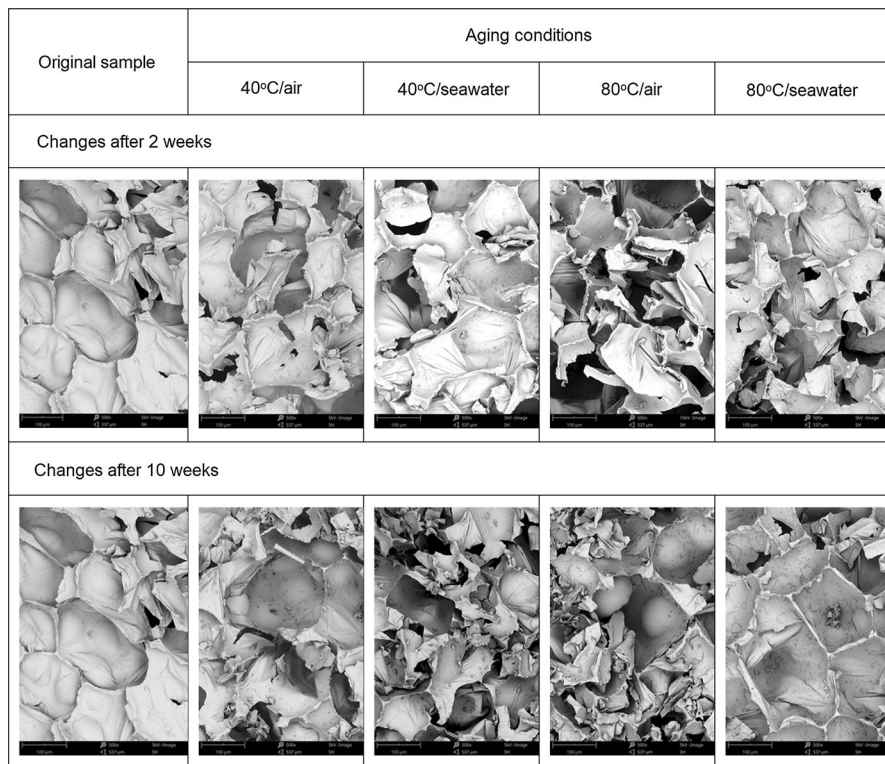

Fig. 12 SEM morphology of the original PU foam and the foam aged at 40 and 80 °C in the air and seawater for 2 and 10 weeks. The images were taken at a magnification of 500x

Samples of aged PU foam were also subjected to testing of mechanical properties: flexural strength, flexural modulus, tensile strength and compressive strength. Figure 13 shows the results of flexural strength tests. The original sample was characterized by the flexural strength of 436 kPa. Aging resulted in the two stage decrease in its values. The first drop was observed after 2 weeks of heating and the achieved value was maintained for the next 4 weeks. The mean value of the flexural strength for samples taken after 2, 4 and 6 weeks of aging was of 399 ± 23 kPa, which corresponds to a 9% decrease in the relation to the flexural strength of the starting material. After a further 2 weeks, a second decrease in the value of flexural strength was observed. The mean value of the flexural strength for samples taken after 8 and 10 weeks of aging was of 361 ± 9 kPa, which corresponds to a 17% decrease in respect to the flexural strength of the starting material. The tests did not show significant differences in the values of the flexural strength with respect to the temperature and aging environment.

Figure 14 shows the results of the flexural modulus tests. The original sample was characterized by a flexural modulus of 4.18 MPa. After the entire duration of the experiment, i.e., 10 weeks, no significant changes in the modulus values were observed. The average modulus value of samples aged in the air was of 4.14 ± 0.37 MPa, which corresponds to the 1% decrease in respect to the starting material. The samples aged in the seawater showed an average modulus value of 3.84 ± 0.27 MPa, which corresponds to the 8% decrease in respect to the starting material.

Figures 15 and 16 shows the results of the tensile strength tests. The original sample showed the tensile strength of 413 kPa. After the first 4 weeks, no changes in its value were observed. The average value of the tensile strength calculated from values shown by samples aged for 2 and 4 weeks in the air and seawater was of 427 ± 27 kPa, which corresponds to the 3% increase in respect to the starting material. In the sixth week of aging, an average 43% increase in tensile strength was observed. Further, aging resulted in the decrease in the tensile strength; however, its average value of 491 ± 44 kPa still was 19% higher than that of the starting material.
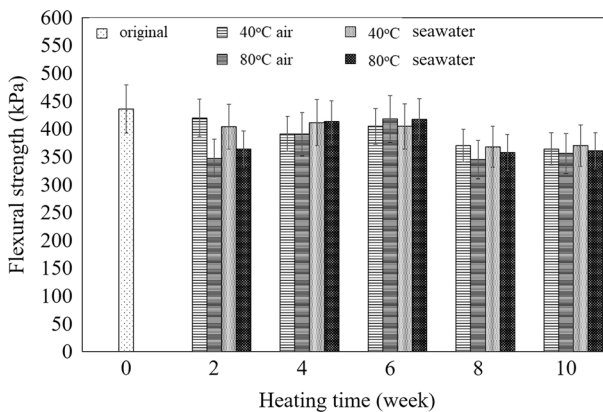

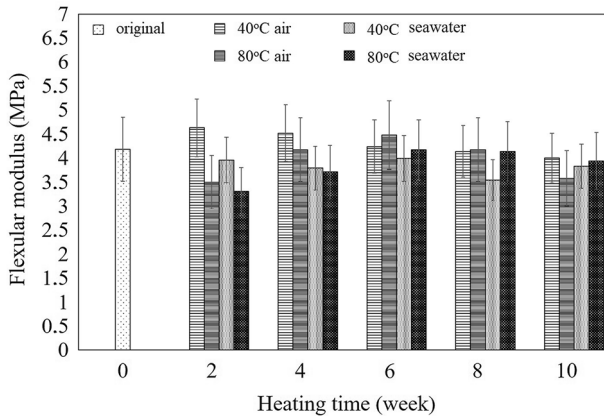**Fig. 13** Flexural strength of an original PU foam and the aged samples

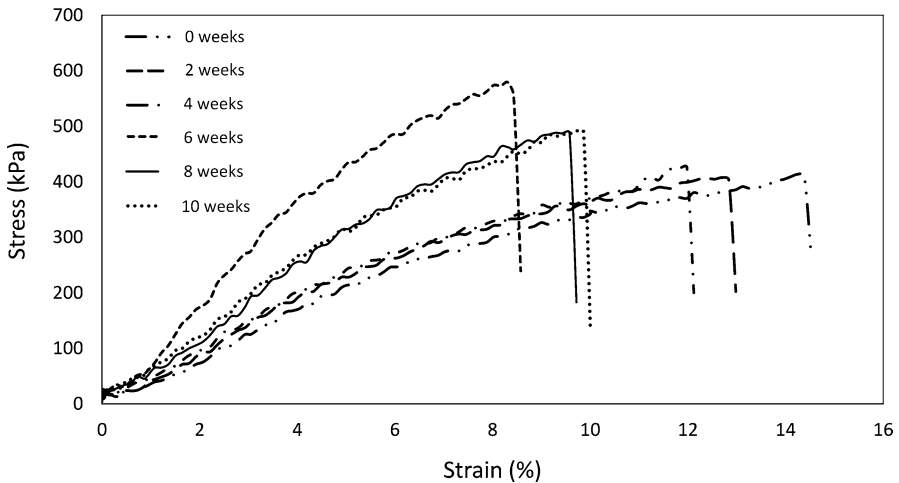**Fig. 14** Flexural modulus of an original PU foam and the aged samples

Fig. 15 Stress–strain graphs for tensile tests of an original PU foam and the samples aged at 40 °C in seawater

Figure 17 shows the results of the compressive strength tests. The original sample showed a compressive strength of 284 kPa. The air-aging for 6 weeks resulted in the compressive strength average value of 307 ± 13 kPa, which corresponded to the average increase of 8% in comparison with the compressive strength of the starting material. Further, aging in the air resulted in the compressive strength decrease, and its average value approached the value measured for the starting material. Seawater had a greater effect on the compressive strength, by decreasing its value. The compressive strength average value of the seawater-aged samples at 40 °C was of 262 ± 17 kPa, which corresponded to 7% decrease in respect to the starting material. In the case of samples aged at 80 °C, the decreases were more radical. The
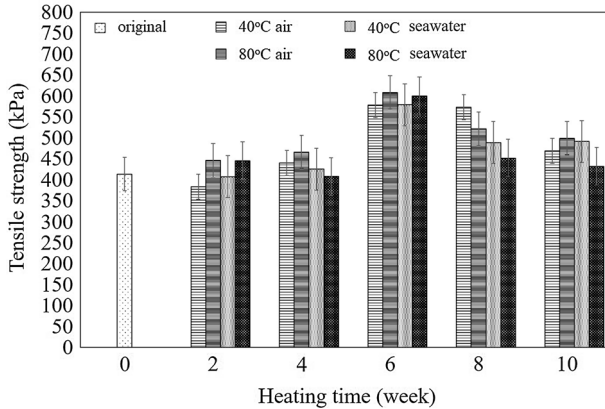
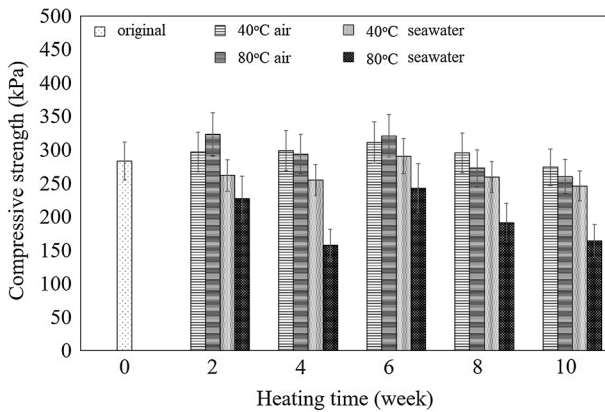**Fig. 16** Tensile strength of an original PU foam and the aged samples

Fig. 17 Compressive strength of an original PU foam and the aged samples

average value of the compressive strength of the seawater-aged samples at 80 °C was of 196 ± 37 kPa, which corresponded to 31% decrease in respect to the starting material.

Discussion

Knowledge about the stability of PU insulation materials at elevated temperatures and various environments is important for the building industry. According to the report of Federation of European Rigid Polyurethane Foam Associations they can be used long-term over a temperature range of -30 to $+90$ °C. Additionally, they can withstand temperatures of up to 250 °C for short periods with no adverse effects [18]. However, there is not much detailed research on this subject. Knowledge of foam stability expressed by various physicochemical and mechanical parameters is

essential for understanding failures of the PU insulations as well as for designing their future applications.

The main purpose of this work was to investigate the response of the commercial closed cell rigid PU foam to severe thermal conditions in two various environments. Samples of the in situ sprayed foam insulation were heated at 40 and 80 °C in the air and seawater for a maximum period of 10 weeks. The foam stability was characterized by monitoring changes in the color, chemical structure, morphology, linear dimensions, mass, water absorption, glass transition temperature, flexural strength and flexural modulus, tensile strength and compressive strength.

Before aging, the PU foam was characterized for its structure. 1H NMR revealed that the studied PU was achieved from MDI (Fig. 1) and polyol (Fig. 2), consisted of EG 23.45 mol% and PG 76.55 mol%. ATR-FTIR confirmed the presence of these structural elements and formation of urethane linkage. Vibrations of the following groups were emerged on the ATR-FTIR spectrum: urethane bonds, aliphatic chains—resulting from the polyol, aromatic rings—resulting from the aromatic diisocyanate (Fig. 11). All components of the urethane linkage –NH–, –C=O and –O– were detected on the ATR-FTIR spectrum in the hydrogen-bonded locations [19, 20]. The SEM analysis confirmed the closed cell PU foam morphology (Fig. 3). The tested material was also checked for solubility in organic solvents, such as chloroform, methylene chloride, acetone, hexane and dimethylsulfoxide. As expected, the foam was insoluble in these solvents. It indicated the PU crosslinked structure, which is typical for rigid PU foams. They are obtained via the polyaddition reaction between polyol and isocyanate of the functionality ≥ 2. Although pure MDI is a difunctional monomer, in fact, in technical applications, it is used in the polymeric form, which provides the monomer functionality from 2.3 to 3.0 [21].

The gradual yellowing of the PU foam was observed due to aging (Fig. 4). It is a well-known phenomenon, which is typically attributed to the photochemical degradation of the polyurethane, caused by UV irradiation [22]. In this study, the UV effect was minimized because the aging was carried out in dark chambers of laboratory ovens. However, samples aged at 80 °C changed their color, from light yellow to yellowish-brown. It indicates that oxidation processes occurred and were more intense at that temperature. It was also noticed that the seawater-aged samples were darker in color than the air-aged samples. In water environment, aromatic amines can be formed in the reaction of the isocyanate group with water [9]. They are easily oxidized to chromophores, which are responsible for the color change of the PU foam [9, 22].

Measurements of linear dimensions were also made in this study (Fig. 5). There is little information in the literature on dimensional changes of PU foams. However, the problem of excessive shrinkage and negative linear changes of PU foams in temperature and humidity conditions were indicated by the researchers [23, 24]. The pressure of the blowing agent inside the foam cells is higher than the atmospheric pressure, which causes its diffusion out of the foam. A diffusion of the blowing agent through the cell walls causes foam shrink [25]. The standards do not specify requirements for dimensional changes of PU foam after production [26, 27]. Therefore, there are no requirements for dimensional stability at ambient temperature for sprayed PU foams. The purpose of the study of Kairytė

et al. was to modify the rigid PET waste-based PU foams in order to achieve foams with improved dimensional stabilities with no more than a 5% change in length and width and 10% change in thickness [28]. The analysis performed in our study revealed that the air-aged samples of the PU foam only slightly changed the diameter and thickness. The average reductions were far below 1%. The sea-water-aging had a more serious effect on dimensional stability. The reduction in diameter and thickness increased exponentially with the aging time. The greater shrinking in the seawater-aged samples can be attributed to the greater diffusion of the blowing agent outside the foam.

The reduction in the sample mass was recorded for the air-aged samples (Fig. 6). The mass reductions can be related to the evaporation of water that naturally occurred in the PU foam due to its hydrophilicity. The temperature of 80 °C resulted in the average mass reduction of 5.36%, which was more than 50% higher than that observed for samples aged at 40 °C. That difference can be assigned to different physicochemical states in which the aging processes were carried out. The tested PU is in the glassy state at a temperature of 40 °C, whereas it is in the viscoelastic state at a temperature of 80 °C (T_g of the original PU sample equals to 59.5 °C). The PU macrochains above the T_g, gained great mobility that eased the migration of water molecules outside the foam.

Knowledge of water absorption is also crucial for the characterization of PU insulations. The seawater-aged samples were tested for this property (Fig. 7). It was observed that WS increased due to aging and that samples aged at 80 °C showed higher WS values than those aged at 40 °C. The WS values after 10 weeks of aging were, respectively, 25 and 15% greater than that shown by the starting foam. As WS of the PU foam depends on the cell size [29, 30], the increases in WS can be explained by the gradual destruction of the cell structure due to the cell opening (Fig. 12), which caused an apparent increase in the cell dimensions. Additionally, greater WS of the samples aged at 80 °C can be attributed to the viscoelastic state of the PU at this temperature. As the PU macrochains have greater mobility in the viscoelastic state than in the glassy state, the water migration is easier in that case.

The results for thermal analysis are shown in Figs. 8, 9, 10. As shown in Fig. 8, the original PU foam showed the T_g of 59.5 °C. It means that the PU constituting the foam occurs in the glassy state at room temperature, which is in agreement with the "rigid" character of the foam. The glass transition was followed by the exother-mic process and next, the endothermic process. The exothermic process can indi-cate a chemical reaction of residual isocyanate groups with polyol hydroxyl groups, whereas the endothermic process can be attributed to a melting of the polymer crys-talline regions. The disappearance of these peaks in the second heating run and the increase in the T_g suggest an increase in the crosslink density. The latter can result from the post-polymerization and/or the formation of hydrogen bonds during the first heating run. The presence of an endothermic peak of lower intensity above 270 °C can be attributed to the decomposition of the urethane bonds and polyol ether bonds [9]. The DSC analysis of aged samples revealed the increases in the T_g due to heating (Fig. 10). Samples aged at 80 °C revealed an average increase in T_g by 80%, whereas those aged at 40 °C revealed an average increase in T_g by 15% in comparison with the T_g of the starting sample. It can be assumed that heating of the

rigid PU foam at 40 °C is safe for its structure and does not increase its stiffness. The temperature of 80 °C can have a more serious effect and can cause PU stiffening.

The aged PU foam samples were also tested for mechanical properties. The stability of mechanical properties is important for construction functionality and safety. Insulation materials made from rigid PU foam are often used in combination with other building materials (for example in external thermal insulation composite systems) for large industrial and agricultural buildings. In such applications, they are exposed to tensile and bending stresses. In certain applications (mostly in flooring), rigid PU foams are exposed to compressive stress, for example, loads that are applied by machines or stored materials [18].

As shown in Figs. 13, 14, 15, 16, tensile strength showed an increasing tendency, flexural strength and compressive strength showed a decreasing tendency, whereas flexural modulus remained unchanged. It could be explained by the chemical crosslink density and the tendency to form hydrogen bonds between urethane bonds. Stirna et al. [21] investigated mechanical properties of rigid PU foams as a function of the polymer molecular weight per branching unit (M_c). (It is described in the literature as the network parameter and is inversely related to crosslink density [31].) They found that tensile strength increased while compressive strength and tensile modulus decreased as the M_c values increased. This was explained by an increasing tendency to form hydrogen bonds with the increasing M_c. It means that the increasing number of physical crosslinks results in the increase in the tensile strength, but does not influence the compressive strength. By analogy, we can assume that heating caused the formation of additional hydrogen bonds, which resulted in the increase in tensile strength. The maximum tensile strength was observed in the sixth week of aging. Later, a small drop was observed, which can be attributed to the degradation of the foam porous structure. Decreases in the flexural strength and compressive strength also can be attributed to the gradual loss of integrity of the porous morphology of the aged samples. As the decreases were greater in the case of the compressive strength, this property can be recognized as the most sensitive mechanical property to aging. It is worth noting that the minimum recorded value of the compressive strength was of 157.7 kPa. This value exceeds 100 kPa, which is sufficient for many rigid PU foam applications [18]. As the flexural modulus remained almost unchanged, this mechanical property can be recognized as the most insensitive to aging at 40 as well as 80 °C in the air and in seawater.

Conclusions

Aging of the rigid PU foam at the temperatures of 40 and 80 °C in the air and seawater for a period of 10 weeks caused changes in the visual appearance, morphology and selected physicochemical as well as mechanical properties. Aging at 80 °C resulted in a sample yellowing, while aging at 40 °C did not bring noticeable color changes. Aging at both temperatures caused deterioration of foam morphology. Its homogeneity decreased due to the cracking of cell edges and ribs. Glass transition temperature increased due to the increasing crosslink density resulting from the post-polymerization and/or formation of hydrogen bonds. The temperature had a much

stronger effect on T_g than the environment and time. Just after 2 weeks of aging, the T_g values increased and achieved a certain level, specific for the particular aging conditions: temperature and environment. The minimum shift of the T_g was observed for the samples aged at 40 °C in the air, which corresponded to a 6% increase in the relation to the T_g of original sample. Greater shifts in T_g were observed for samples heated at 80 °C, which corresponded to an almost twofold increases. Water absorption also increased due to aging. Samples aged at 80 °C showed higher WS values than those aged at 40 °C. The WS values after 10 weeks of aging were, respectively, 25 and 15% greater than that shown by the starting foam. These increases can be attributed to the partial cell opening in aged samples. As the PU macrochains have greater mobility in the viscoelastic state than in the glassy state, the water migration was easier at 80 °C.

The flexural strength and compressive strength showed a decreasing tendency with aging time. The maximum shift of flexural strength from 436 to 345 kPa was observed after 8 weeks of aging in the air at 80 °C. The maximum shift of compressive strength from 284 to 158 kPa was observed after 4 weeks of aging in seawater at 80 °C. These decreases can be assigned to the degradation of the porous morphology. On the other hand, aging caused an increase in the tensile strength, probably due to the increase in the physical crosslink density. The starting material was characterized by the tensile strength of 413 kPa. Its highest value was of 608 kPa, and it was observed after 6 weeks of aging in the air at 80 °C. The changes in modulus were statistically insignificant and its average value was of 4.0 MPa.

Declaration

Conflict of interest The authors declare that there is no conflict of interest.

References

1. Malewska E, Sabanowska A, Polaczek J, Prociak A (2012) Physical and mechanical properties of rigid polyurethane foams modified with polystyrene beads. E-Polymers 12(1). Doi: https://doi.org/10.1515/epoly.2012.12.1.637.

2. Magrini A (2014) building refurbishment for energy performance: a global approach. Springer Science & Business Media, Berlin

3. Demharter A (1998) Polyurethane rigid foam, a proven thermal insulating material for applications between +130 °C and −196 °C. Cryogenics 38(1):113–117. https://doi.org/10.1016/S0011-2275(97)00120-3

4. Radziszewska-Zielina E (2009) Analiza porównawcza parametrów materiałów termoizolacyjnych mających zastosowanie jako izolacja ścian zewnętrznych. Przegląd budowlany 4:32–37

5. Pfundstein M, Gellert R, Spitzner M, Rudolphi A (2007) Insulating materials: principles, materials, applications. Institut für Internationale Architektur-Dokumentation. An Edition Detail book. 1st edn. Munich pp. 96. A. Rudolphi. Insulating materials from the ecological viewpoint. pp 93–113.

6. Przewoźnik A (2014) Polyurethane—alternative to mineral wool and polystyrene Czasopismo Techniczne. Budownictwo 5-B:229–233

7. Marrucho IM, Santos F, Oliveira N, Dohrn R (2005) Aging of rigid polyurethane foams: thermal conductivity of N_2 and cyclopentane gas mixtures. J Cell Plast 41:207–224. https://doi.org/10.1177/0021955X05053520

8. Davies P, Evrard G (2007) Accelerated ageing of polyurethanes for marine applications. Polym Degr Stab 92(8):1455–1464. https://doi.org/10.1016/j.polymdegradstab.2007.05.016

9. Liszkowska J, Moraczewski K, Borowicz M, Paciorek-Sadowska J, Czupryński B, Isbrandt M (2019) The effect of accelerated aging conditions on the properties of rigid polyurethane-polyisocyanurate foams modified by cinnamon extract. Appl Sci 9:2663

10. Liszkowska J, Borowicz M, Paciorek-Sadowska J, Isbrandt M, Czupryński B, Moraczewski K (2020) Assessment of photodegradation and biodegradation of RPU/PIR foams modified by natural compounds of plant origin. Polymers (Basel) 12(1):33. https://doi.org/10.3390/polym12010033

11. ASTM standard: D1141 (1998) Standard practice for the preparation of substitute ocean water

12. ISO standard: ISO 1923 (1981) Cellular plastics and rubbers—determination of linear dimensions

13. ISO standard: ISO 2896 (2001) Rigid cellular plastics—determination of water absorption

14. ISO standard: ISO 11357-2 (2020) Plastics—differential scanning calorimetry (DSC)—part 2: determination of glass transition temperature and step height

15. Polish standard: PN-EN 12089 (2013) Thermal insulating products for building applications—determination of bending behavior

16. Polish standard: PN-EN 1608 (2013) Thermal insulating products for building applications—determination of tensile strength parallel to faces

17. Polish standard: PN-EN 826 (2013) Thermal insulating products for building applications—determination of compressive behavior

18. Federation of European Rigid Polyurethane Foam Associations (2006) Thermal insulation materials made of rigid polyurethane foam. (PUR/PIR). Properties—manufacture. Report No. 1, October 2006. http://highperformanceinsulation.eu/wp-content/uploads/2016/08/Thermal_insulation_materials_made_of_rigid_polyurethane_foam.pdf

19. Wong C, Badri K (2012) Chemical analyses of palm kernel oil-based polyurethane prepolymer. Mater Sci Appl 3(2):78–86. https://doi.org/10.4236/msa.2012.32012

20. Mutsuhisa F, Ken K, Shohei N (2007) Microphase separated structure and mechanical properties of norbornane diisocyanate-based polyurethane. Polymer 48(4):997–1004. https://doi.org/10.1016/j.polymer.2006.12.057

21. Stirna U, Beverte I, Yakushin V, Cabulis U (2011) Mechanical properties of rigid polyurethane foams at room and cryogenic temperatures. J Cell Plast 47(4):337–355. https://doi.org/10.1177/0021955X11398381

22. Rosu D, Rosu L, Cascaval CN (2009) IR-change and yellowing of polyurethane as a result of UV irradiation. Polym Deg Stab. 94(4):591–596. https://doi.org/10.1016/j.polymdegradstab.2009.01.013

23. Kurańska M, Prociak A (2016) The influence of rapeseed oil-based polyols on the foaming process of rigid polyurethane foams. Ind Crops Prod 89:182–187. https://doi.org/10.1016/j.indcrop.2016.05.016

24. Hejna A, Kirpluks M, Kosmela P, Cabulis U, Haponiuk J, Piszczyk Ł (2017) The influence of crude glycerol and castor oil-based polyol on the structure and performance of rigid polyurethane-polyisocianurate foams. Ind Crops Prod 95:113–125. https://doi.org/10.1016/j.indcrop.2016.10.023

25. Zhang J, Hori N, Takemura A (2019) Optimization of preparation process to produce polyurethane foam made by oilseed rape straw based polyol. Polym Degrad Stab 166:31–39. https://doi.org/10.1016/j.polymdegradstab.2019.05.022

26. EN 13165 (2016) Thermal insulation products for buildings—factory made rigid polyurethane foam (PU) products—specification. European Standardization Committee, Brussels

27. EN 14315-1 (2013) Thermal insulating products for buildings—in-situ formed sprayed rigid polyurethane (PUR) and polyisocyanurate (PIR) foam products—part 1: specification for the rigid foam spray system before installation. European Standardization Committee, Belgium

28. Kairytė A, Kremensas A, Balčiūnas G, Członka S, Strąkowska A (2020) Closed cell rigid polyurethane foams based on low functionality polyols: research of dimensional stability and standardised performance properties. Materials 13:1438. https://doi.org/10.3390/ma13061438

29. Kurańska M, Prociak A, Kirpluks M, Cabulis U (2013) Porous polyurethane composites based on bio-components. Compos Sci Technol 75:70–76. https://doi.org/10.1016/j.compscitech.2012.11.014

30. Brenes D, Cubero-Sesin J, Orozco F, Vega-Baudrit J, Gonzalez-Paz R (2017) Variation of physical properties of rigid polyurethane foams synthesized from renewable sources with different commercial catalysts. J Renew Mater. 5(3). Doi: https://doi.org/10.7569/JRM.2017.634118.

31. Barszczewska-Rybarek I, Korytkowska A, Gibas M (2001) Investigations on the structure of poly(dimethacrylate)s. Des Monom Polym 4(4):301–314. https://doi.org/10.1163/156855501753210790

Publisher's Note Springer Nature remains neutral with regard to jurisdictional claims in published maps and institutional affiliations.